

September 22, 2010

MEMORANDUM TO: Jack Guttman, Branch Chief
Performance Assessment Branch, HLWRS

FROM: Tianqing Cao, Senior Seismologist **/RA/**
Repository Site Branch, HLWRS

SUBJECT: YUCCA MOUNTAIN CONFIRMATORY DRIFT DEGRADATION
CALCULATIONS

As part of my postclosure drift degradation review I performed some confirmatory calculations.

Short Abstract

My calculation shows:

- (1) The mechanical stress disturbance due to tunnel excavation diminishes at around two tunnel radiuses from the center of the opening.
- (2) The excavation creates low stress zones near crown and floor areas and high stress zones near sidewalls. The rock strength is higher than the stress around the opening and no spalling will occur without thermal stress added on.
- (3) Thermal stress is mostly tangential. When it is added to the mechanical stress the thermoelastic stress can cause spalling.
- (4) Spalling will most like to occur near crown area because the low radial confining or tensile stress there. Spalling will start from a small area where the combination of stress and rock strength heterogeneities is most susceptible to spalling.
- (5) Spalling itself releases the lateral (tangential) stress and prevents further spalling in the lateral directions. The only direction for spalling to progress is deeper into the rock where the confining stress is higher and tangential stress lower which makes further spalling harder. So spalling area will gradually shrink and reach self-rest before two radius distance from the center of the opening.
- (6) The added thermal stress may make spalling possible if the mechanical stress alone is not enough. But the time dependent thermal loading only changes the pace of spalling not the scale of spalling because the scale of the initial spalling is determined by the heterogeneities of rock strength and loaded stress. Once spalling occurs it cannot extend laterally due to lateral stress release by spalling itself. It can only go deeper before reaching self rest.

CONTACT: Tianqing Cao, NMSS/HLWRS
(301) 492-3568

Long Abstract

In order to study the stress condition around a circular tunnel and the rock spalling process, I followed some practical guidelines in rock mechanics and adopted an elastic model because the zones of inelastic response are small. I found that the stress disturbance due to excavation reaches to about two radiuses from the center of the opening. When the tunnel is heated to 150° C the thermoelastic stress near some part of the opening exceeds the rock strength. But at two radiuses distance from the tunnel center the stress is still well below the confined rock strength.

The opening creates very different mechanical stress conditions (patterns) in different areas near the opening surface. The rock near the sidewalls is under triaxial compression (confined condition) and the strength becomes a few times higher than the unconfined uniaxial compressive strength. The rock near the crown and floor areas is under biaxial condition in which the radial stress is very low or tensile. The rock there is squeezed in tangential and axial directions and allowed to go in the radial direction. The thermal stress is mostly tangential. When the squeezing stress is high enough the rock can be peeled off and causes spalling. Tension or very little compression in the radial direction is a necessary condition for where spalling occurs first.

The level of tangential stress, mechanical and thermal, determines when spalling will occur. It always occurs at a small area first because of rock strength heterogeneity, existing cracks, and nonuniform stress. Spalling can occur repeatedly because each spalling exposes the inside rock to the similar stress condition for spalling. However, each spalling only creates a smaller crown area above for the next spalling and releases the tangential stresses around the spalling block to prevent further spalling in the lateral (tangential) directions. This process of deepening and narrowing will stop after the spalling tip reaches a well confined stress condition where the rock strength is a few times of the unconfined strength but is within two radius distances from the center as calculated and observed.

The heating increases the tangential stress significantly but much less the radial stress because the heating cause rock expansion near the opening surface and the radial direction is free to expand. The added thermal stress will change when to spall but not extend where to spall in the tangential directions. This is equivalent to say that thermal stress will not increase the total amount of spalling but will shorten the time needed to cumulate that amount. The horizontal to vertical stress ratio (k value) has some influence on the mechanical stress distribution near the crown and floor areas especially in the radial direction. A small value ($<1/3$) will lead to a radial and tangential tension zone near the crown and floor areas which reduces the rock strength significantly and increases the chance of spalling. A smaller k value will also make the spalling region bigger. A higher k value (0.5) used by DOE may have resulted in less chance of spalling and smaller region of spalling compared with a value of 0.25 used by Ofoegbu et al. (2007).

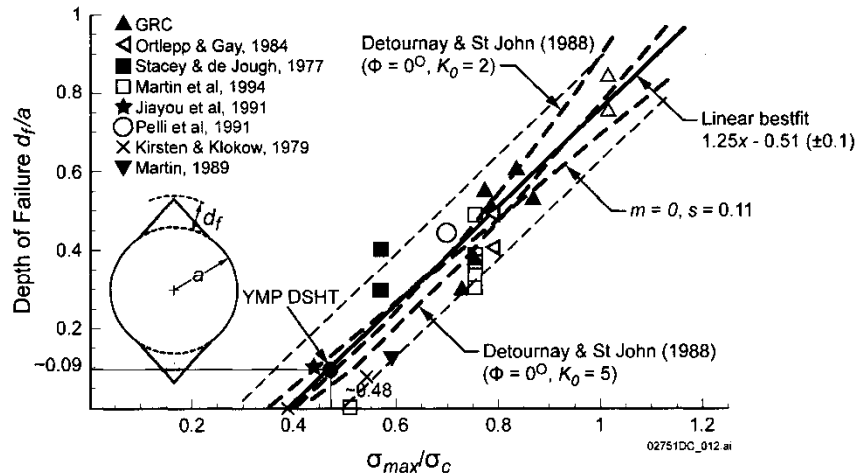
Introduction

I will introduce some observational and modeling results on rock spalling first and then present some of the fundamentals on rock stress and strength. The elastic modeling adopted in this study is followed by the thermal stress calculation. Finally in the discussion section I summarize the modeling results and provide answers to those questions related to rock spalling.

(A) Some Observational and Modeling results

A few observational and modeling results are directly related to the drift degradation, especially spalling:

- 1) **Spalling and heating.** Most of the observed spalling was from underground tunnels without heating. Spalling happens near the crown and floor (heap) areas of a tunnel. Shallow fractures are observed on the sidewalls.
- 2) **Observed spalling depth.** Martin et al. (1999) performed a review of observed depths of failure from “overstressed” tunnels in mines worldwide and determined the depth of failure is linearly related to the ratio between the maximum tangential stress and the laboratory uniaxial unconfined compressive strength (see DOE RAI response 3.2.2.1.2.1, page 6 of 11). Kaiser et al. (2000) showed that from sedimentary siltstones to igneous granites including case examples in which the value of maximum tangential stress is greater than the uniaxial unconfined compressive strength of the rock a depth of failure of slightly less than **one tunnel radius** before self-stabilization of the tunnel geometry (see Fig. 1). Kaiser et al. (2000) did not indicate if thermal heating was involved in the data.
- 3) **DOE’s heating experiment and modeling.** After less than 4 years of heating in the DOE’s Drift Scale Heater Test spalling at several locations in the crown of the tunnel was observed (BSC, 2004, page7-45). DOE’s numerical modeling for 10 years of heating shows that the calculated tangential stress, which is used by DOE and Center to be compared with the unconfined compressive strength to determine overstress and failure, is still much higher near the sidewalls than near the crown and heap areas (BSC, 2004, page 6-52). The modeling shows that after 100 years of heating the tangential stress near the crown area has increased to be slightly higher than near the sidewalls.
- 4) **Rock strength and confining stress.** Compressional rock strength increases dramatically under triaxial compression or large confining stress. Figure 2 is an example from Brady and Brown (1985, page 111) to show such increases. This figure shows that with a confining stress of 20% of the unconfined rock strength, the confined strength is about twice of the unconfined strength; the confined strength is tripled when the confined stress increases to about 50% of the unconfined strength.
- 5) **Thermal stress and mechanical stress.** The total tangential stress with the thermal stress included will reach a level of slightly more than **twice** of the mean unconfined compressive strength for high-grade lithophysal rock at the crown area and a level about the mean strength at sidewall according to (Ofoegbu et al., 2007). This requires much higher heating near the crown area than the sidewall area because the mechanical stress at sidewall area is higher than the crown area. This higher heating near the crown area is different from DOE’s (Fig. 6-140, BSC, 2004) thermal model and Manepally et al.’s (2004) thermal model which predict the temperature at crown area is lower than the sidewall area by 20° C at the time when the drift reaches the highest postclosure temperature.



Source: Kaiser et al. 2000, Figure 3.12.

Figure 1. Relation of the depth of failure as a function of the maximum boundary stress to uniaxial compressive strength ratio for tunnels in hard rock (quoted by RAI response of 3.2.2.1.2.1-006, on page 3 of 7).

Some of the interesting questions we wish to answer are as following:

- 1) Why does spalling occur near crown and floor (heap) areas where the tangential stress is lower than the sidewall areas?
- 2) Is the failure criterion to compare the tangential stress with the uniaxial unconfined strength appropriate?
- 3) Why is the observed worldwide maximum spalling depth (Kaiser et al., 2000) about one radius?
- 4) Should spalling with thermal stress added continue or stop at certain depth?

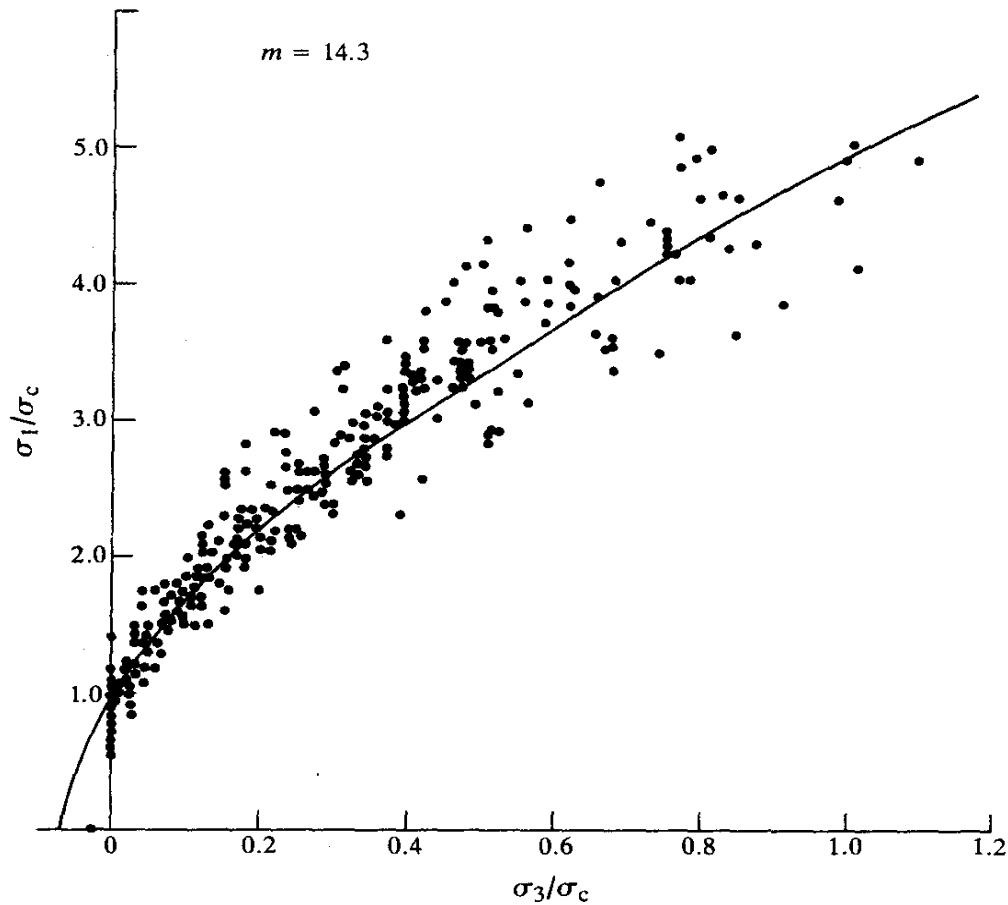


Figure 2. Normalized (by the unconfined uniaxial strength) peak strength envelope for sandstones (after Hoek & Brown 1980).

(B) Rock Strength and Failure in Different Stress Conditions

In rock mechanics, three principal stresses, $\sigma_1 \geq \sigma_2 \geq \sigma_3$ are called major, intermediate, and minor principal stresses. The typical stress conditions are (a) biaxial compression ($\sigma_1 \geq \sigma_2, \sigma_3 = 0$), which is the stress condition around the excavation opening surface, (b) triaxial compression ($\sigma_1 > \sigma_2 = \sigma_3$), (c) polyaxial compression ($\sigma_1 > \sigma_2 > \sigma_3$), and uniaxial compression, which is not a case found around an excavation. It is useful in the following discussions to notice that the rock strength increases greatly when σ_1 increases from zero (biaxial) to greater than $\sigma_2 = \sigma_3$ (triaxial). Figure 2 is an example from sandstone experiments to show such strength increase. The opposite is also true that the rock strength decreases greatly when σ_1 decreases from zero to negative (tension).

The fracture modes for the uniaxial compression are local tensile fracture predominantly parallel to the applied stress and local and macroscopic shear fracture or faulting (Brady and

Brown, 1985, page 96). For biaxial compression and $\sigma_2 = \sigma_1$, no strength increase was observed or the 'strengthening' effect of the intermediate principal stress can be neglected so that the uniaxial compressive strength σ_c should be used (Brady and Brown, 1985, page 101). The rock is being squeezed under biaxial compression and driven to the zero stress direction. The fracture mode under biaxial compression is more likely to be spalling. Rock under uniaxial tension fail at stresses an order of magnitude lower than when tested in uniaxial compression (Brady and Brown, 1985, page 5).

The stress condition around a circular excavation is biaxial on the opening surface because of the zero radial stress and triaxial compression going inward from the opening because of the nonzero compressive radial stress. The details of the stress distribution will be presented in the next section.

(C) Radial and Tangential Stress Distributions around an Excavation

In order to study the stress distribution around an excavation and shed light on rock spalling I follow the guideline in rock mechanics that "some useful engineering insights into the behavior of excavation peripheral rock can be established by exploiting quite simple conceptual (elastic) models of the effects of inelastic deformation" (Brady and Brown, 1985, page 194). The elastic model is also justified to be used because the zones of inelastic response are small relative to the dimensions of the excavation. Many results, such as where spalling will occur, are indicated by the stress distribution of an elastic model without modeling the process to include failure.

Figure 3 is from Brady and Brown (1985) to show a long excavation (tunnel) with p representing the overburden vertical stress and kp the horizontal stress. Here k represents the stress ratio between horizontal and vertical. It is obvious that large k means higher horizontal stress and more support to the vertical load. The vertical in situ stress p is determined by the depth of the tunnel and the density of the overburden rock. The horizontal stress is about a half of the vertical stress p when the Poisson ratio of 0.2 is chosen (BSC, 2004, page 6-59). The stress distribution around this excavation is a 2-D elastic problem and was solved by Kirsch in 1898 (Brady and Brown, 1985, page 162). Along the radial lines at $\theta = 0^\circ$ and $\theta = 180^\circ$ (horizontal) and at $\theta = 90^\circ$ and $\theta = 270^\circ$ (vertical), shear stress $\sigma_{r\theta} = 0$ and the three principal stresses are radial stress σ_{rr} , tangential stress (hoop) $\sigma_{\theta\theta}$, and the third stress along the tunnel direction (axial stress, not shown in Fig. 3).

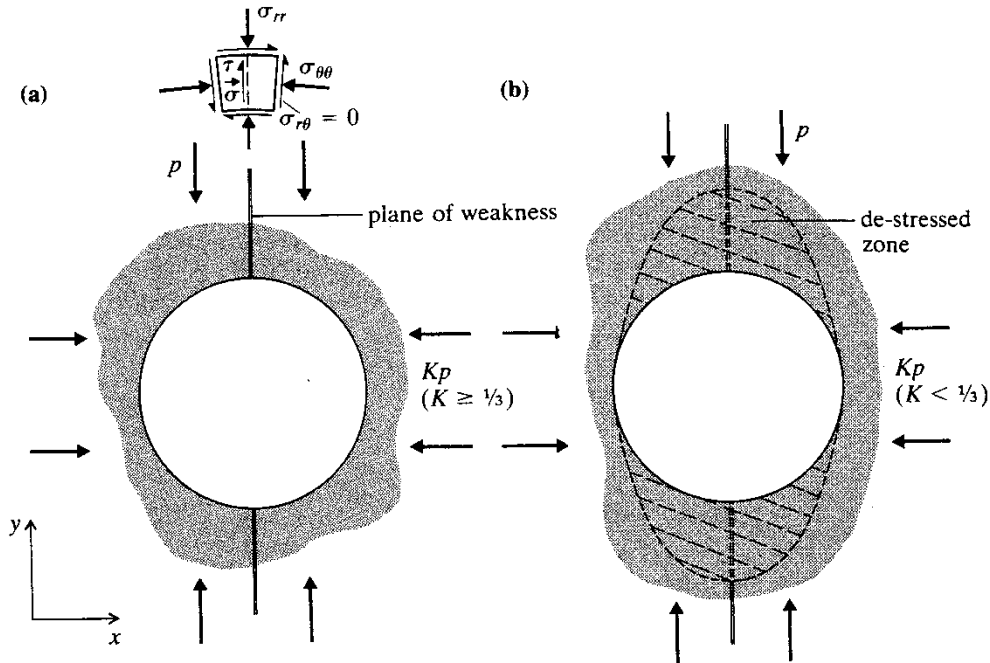


Figure 3. A cross section of an excavation with vertical and horizontal stresses p and kp . K is the stress ratio between vertical and horizontal (from Brady and Brown, 1985, page 190).

Stress behind the opening

The radial and tangential stresses along the lines from the center of the tunnel perpendicular to the sidewall and crown are calculated with Kirsch's formulas using $k=0.5$ and shown in Figures 4 and 5. In Figs. 4 and 5, the distance r from the tunnel center is normalized by the tunnel radius a and the stress S (σ_{rr} or $\sigma_{\theta\theta}$) is normalized by the vertical stress p .

Similar kind of radial stress plot was used to analyze the stability under the divergent wave loading (BSC, 2004, Figure 7-59). But we are here to analyze the stress conditions of the rock surrounding the tunnel opening.

The observations of stress distribution from Figs. 4 and 5 are:

- 1) Radial stress is compressional with $k=0.5$ at all distances and increases from zero at the tunnel surface ($r/a=1.0$) into the rock media (Fig. 4). The increase is much faster into the sidewalls than into the crown and floor. According to the strength and stress analyses in the last section, this faster increase into the sidewalls means that the confined rock strength inside the sidewalls is higher than inside the crown and floor at the same distance from the center. This may explain why fracturing is less likely to progress in the sidewall direction.
- 2) The two curves in Fig. 4 cross each other around $r/a=1.75$. After the crossing, the radial stress in the crown direction is compatible to the area inside the sidewall at same distance to the center. From Figs. 4 and 5, it is clear that at distances large than two radius ($r/a>2$) the stress distributions almost return to the condition without excavation. In another word, the stress disturbance of excavation reaches to about one tunnel radius beyond the excavation. The stress condition deep inside crown area ($r/a>2$) is triaxial compression with the radial stress greater than the two equal horizontal stresses, one tangential and the other axial. The stress inside the sidewall ($r/a>2$) is also triaxial

compression with the vertical stress as the major principal stress and the two equal horizontal (tangential and axial) stresses as the confining stresses. We have shown that under the triaxial compression the rock strength increases dramatically (Fig. 2). This may explain the observed worldwide rock spalling data (Fig. 1), which show that the spalling depth is limited to about one tunnel radius.

- 3) The stress condition near the crown area is biaxial compression for $k=0.5$. When using $k=0.25 < 1/3$, as indicated in Fig. 3 (b), there is a layer from $r/a=1.0$ to $r/a=1.06$ under radial tension (see Fig. 6). It is called the de-stressed zone in Fig. 3 (b). The tangential stress here in a region about 15 degrees to each side of the vertical direction also becomes tensile. This is the ideal condition for rock spalling because tension reduces the rock strength. For a tunnel of radius $a=2.5$ m, this layer is 15 cm thick with the most likely break point at the middle of this layer ($r/a=1.03$) where the tension in vertical (radial) direction is the highest. So the spalling thickness is around 7.5 cm. Of course, when k increases to greater than $1/3$ the tension will become very low compression and the crown area remains to be the most susceptible region for spalling when compared to other areas around the tunnel opening.
- 4) Fig. 5 shows that the tangential stress near the sidewall is much higher than near the crown. This may explain why fractures are observed first on the sidewalls right after the excavation in DOE's heating experiment tunnel. Such high tangential stress decreases quickly inward and the compressive stress in the radial direction increases. These two changes result in the strength increase and preventing further fracturing.

Stress near the opening

Although Figs. 4 and 5 have revealed the stress conditions inside of the crown and sidewall areas and may explain the range that fracturing and spalling may reach, it has not provided the information about to what extent the fracturing and spalling will occur and if it will ever stop.

Figures 7 and 8 are plots of radial and tangential stresses as a function of azimuth theta. In each figure, three distances from the center are included to show the stress change inward from the opening. Fig. 7 shows that the compressive radial stress is lowest near the crown area, which is in favor of spalling. But such low compressive (for $k < 1/3$, it will be tensile) area only expands about ten to fifteen degrees on each side of the vertical line ($\theta = 90^\circ$) and to a very shallow depth (about 6% of the radius, see Fig. 6). This is the most likely area for spalling to start (Brady and Brown got 11 degrees for $p=7.5$ MPa and $k=0.3$ for the tensile region, see page 199). Fig. 8 shows that this area is experiencing tangential (squeezing) stress which is low near opening surface and high inward up to about 1.2 radius (see Fig. 5). This type of stress condition is in favor of squeezing out. For the sidewall area the opposite is true (see Figs. 8 and 5). Figs. 6 and 7 show that the low compressive or tensile ($k < 1/3$) radial stress is the measure for determining the extent of potential spalling.

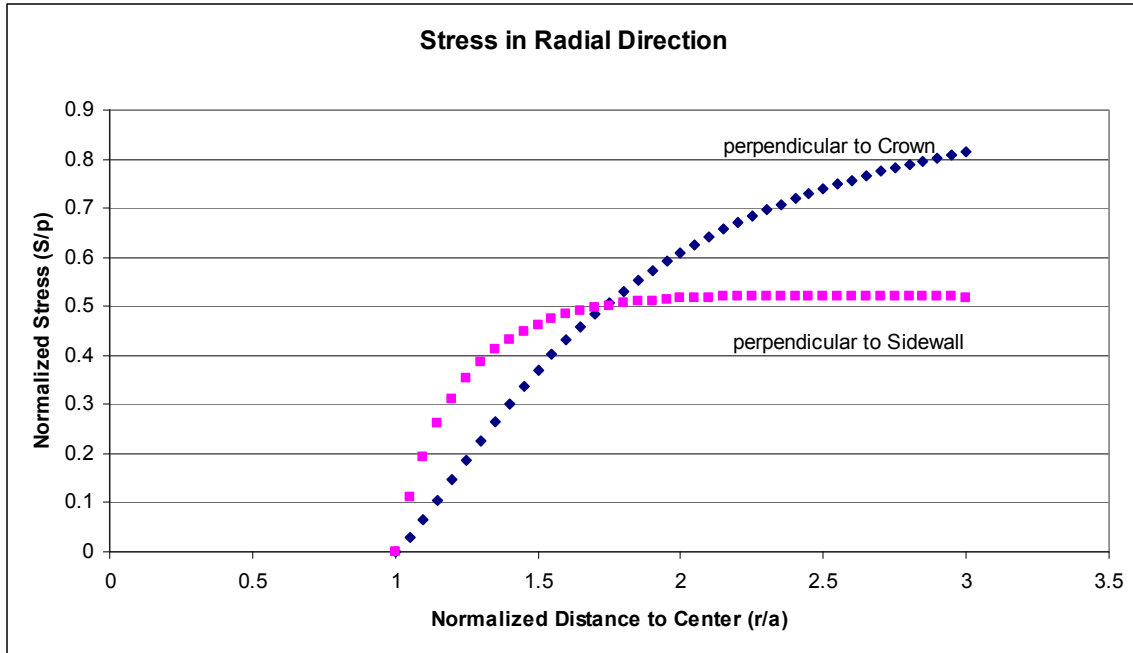


Figure 4. Radial stresses along the radius perpendicular to crown or sidewall of a tunnel, which are normalized by the vertical in situ stress ρ . The distance r from the center of the tunnel is also normalized by the tunnel radius a .

The exact extent of this small region for spalling to start is not very important. Once the spalling starts, it will expose the rock inside above the crown area to similar stress condition (but higher radial and lower tangential compressions, see Figs. 4 and 7) and cause new spalling. It will also release the tangential stress in a ring surrounding the tunnel opening with a thickness approximately equal to the spalling depth and prevent more spalling in the lateral (tangential) directions. This means the spalling area becomes narrower each time when spalling progresses deeper into the rock. This narrowing process may explain the cone shape of spalling areas in Fig. 1 and why spalling eventually will stop when the front becomes so narrow it is well confined.

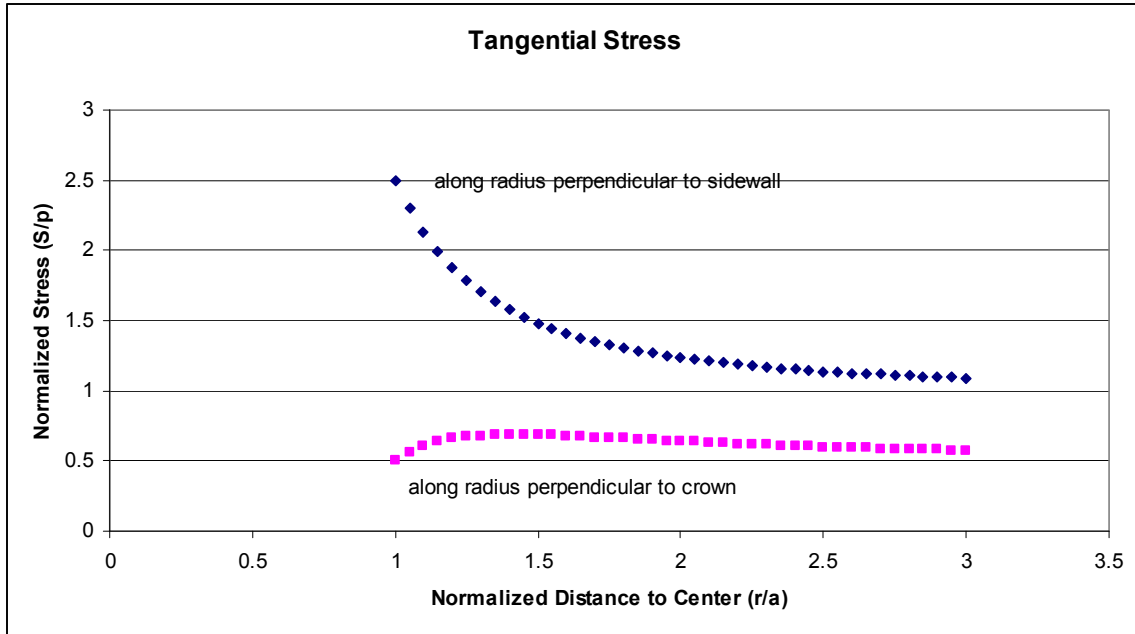


Figure 5. Tangential stresses along the radius perpendicular to crown or sidewall of a tunnel, which are normalized by the vertical in situ stress p . The distance r from the center of the tunnel is also normalized by the tunnel radius a .

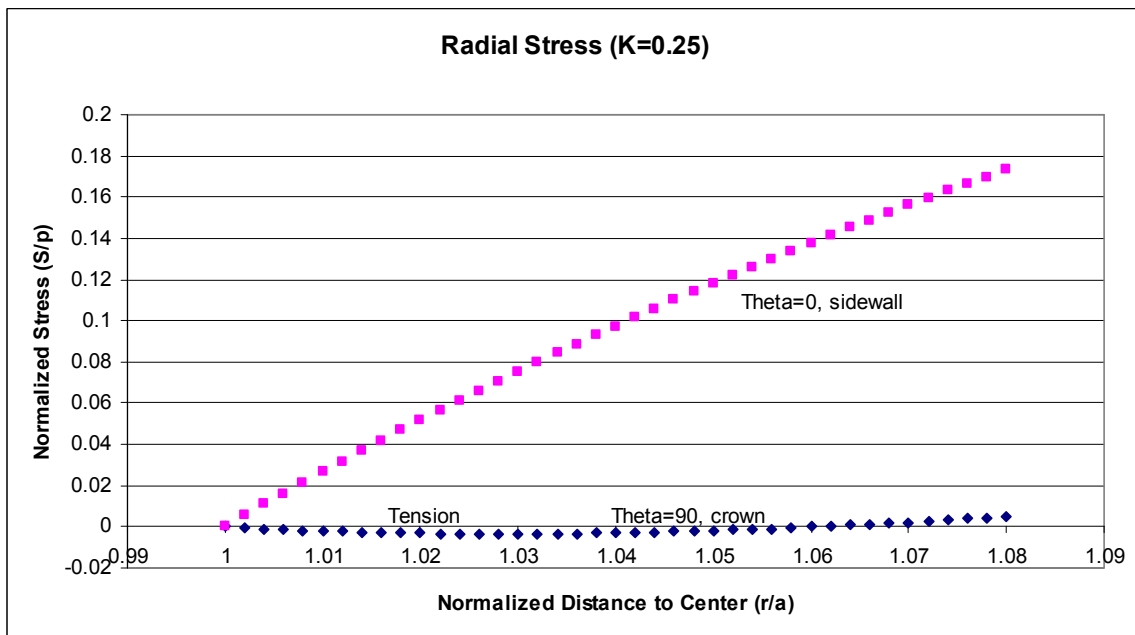


Fig. 6. Radial stress with $k=0.25$ to show a tension layer from $r/a=1.0$ to $r/a=1.06$ in the crown area above the tunnel surface.

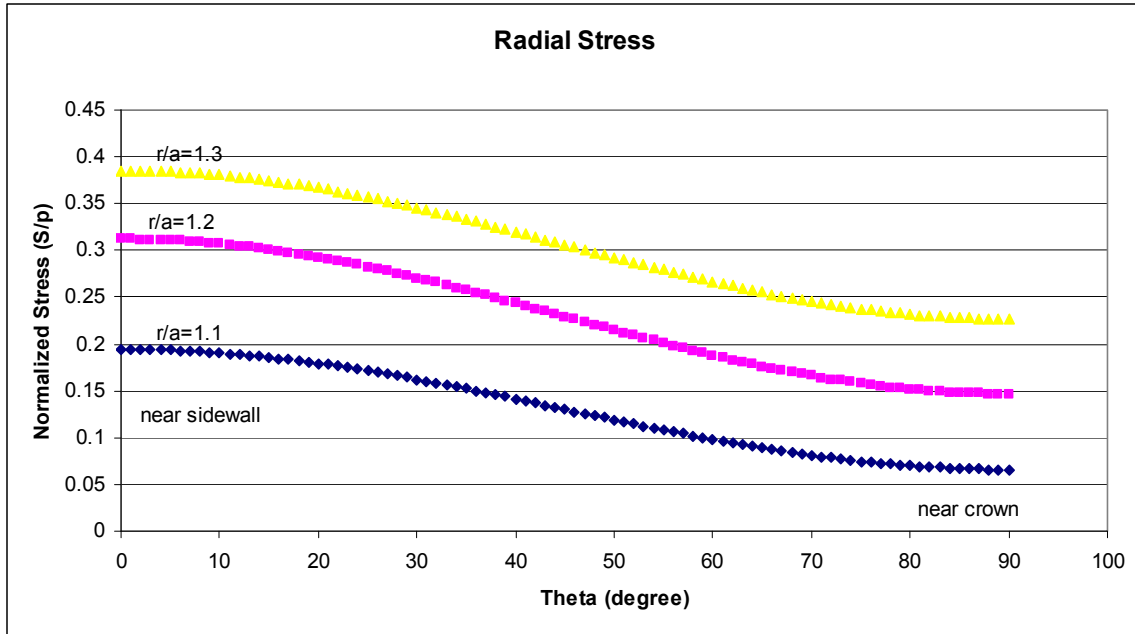


Figure 7. Radial stresses ($k=0.5$) for three r/a ratios as a function of azimuthal angle theta.

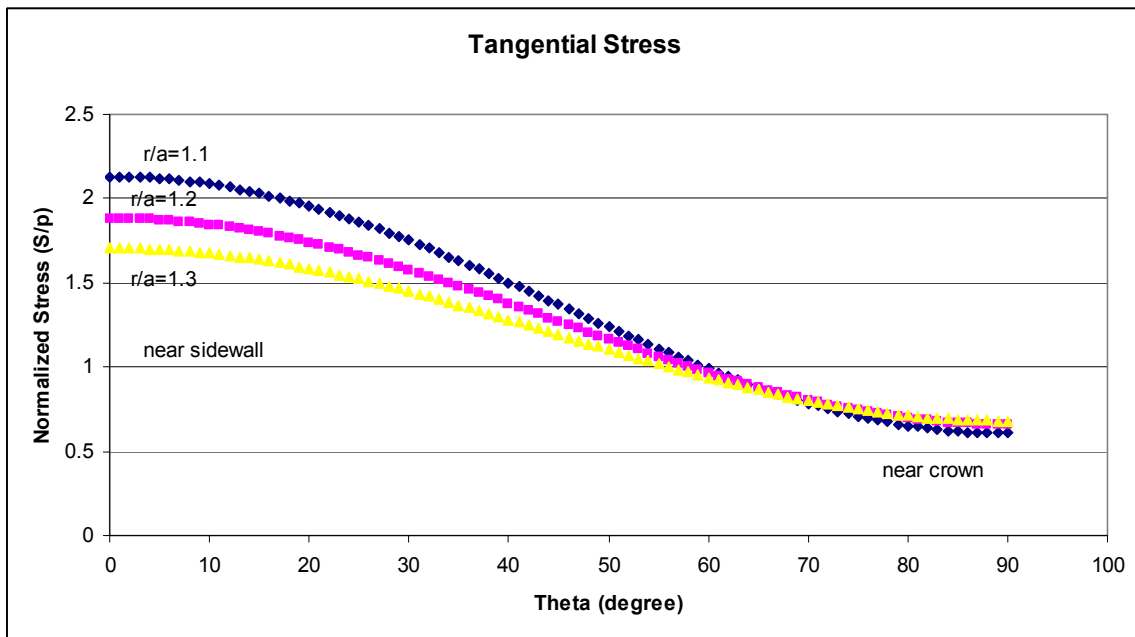


Figure 8. Tangential stresses ($k=0.5$) for three r/a ratios as a function of azimuthal angle theta.

Because of the symmetry, the opposite side from the crown area, the floor (heap) area should be under the similar stress condition like the crown area and also susceptible to spalling according the above calculation, which is actually observed worldwide (see Fig. 1).

For a heated tunnel, the crown area will be hotter than the floor area so the tangential stress at crown area will be higher than the floor area. The spalling process here will be faster.

(D) Thermoelastic Stress Distribution

This section discusses the stress distribution around the cylindrical opening with inside heating. The heating history is not calculated here. We are more interested in the thermal effect on stress distribution. We use a fixed high temperature (150°C, see BSC 2004, page 6-51) at the drift surface from DOE’s calculated drift temperature history and calculate the thermoelastic stresses around the drift. The temperature distribution is assumed only dependent on the radial distance from the drift center. We assume the temperature decays with the distance (r) from the center and is proportional to $1/r$.

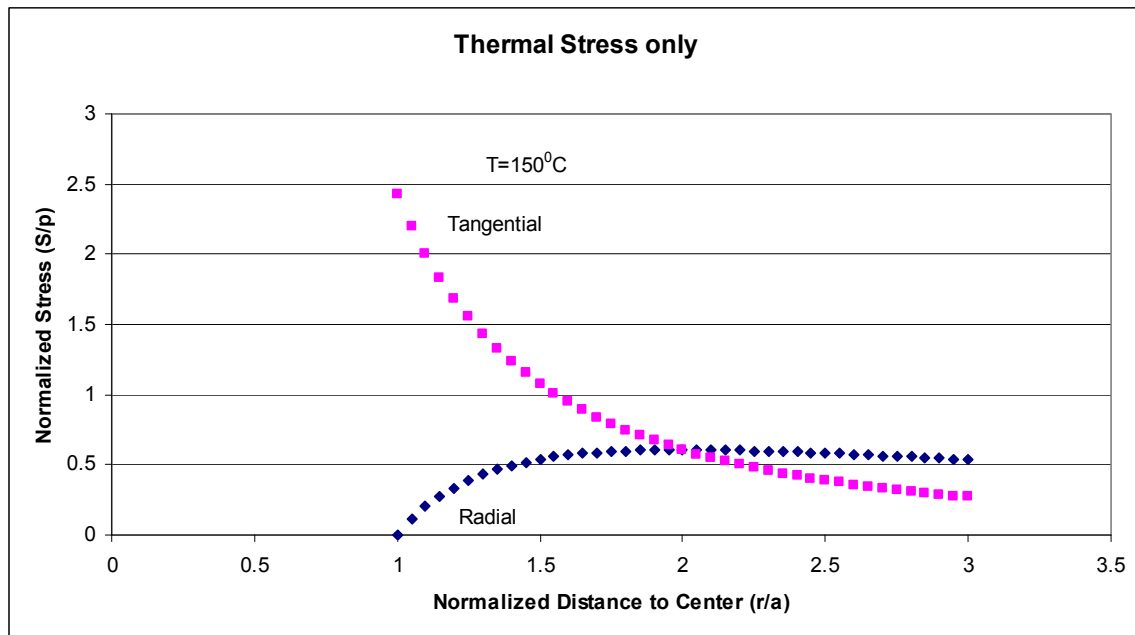


Figure 9. The tangential and radial thermal stresses along the vertical line from the center of the drift (Theta=90 degree, crown).

The formulation for thermoelastic stress and its solution with the above assumptions are presented in Appendix A. The parameters needed for the part of thermal stress calculation are Young’s modulus, the coefficient of linear thermal expansion, and the vertical in situ stress p . The Young’s modulus is 10 GPa (Table 1, Ofoegbu et al. 2007), thermal expansion coefficient is 9.07×10^{-6} , which is for temperature greater than 100°C (BSC 2004, page C-9), and the vertical stress p is 7 MPa (BSC 2004, page 6-59).

Figure 9 shows the tangential and radial thermal stresses along the vertical line (Theta=90 degree) from the center of the drift.

In order to compare with the mechanical stresses we plotted the tangential and radial mechanical stresses in Figure 10. It is clear that the tangential stress increases significantly lot especially in the area very near the opening (r close to 1).

Figure 11 shows the thermoelastic stress for a temperature 150°C on the opening surface. Now the tangential stress has reached the level of three time of the vertical in situ stress p , which is 21 MPa or about the uniaxial unconfined rock strength (Table 1, Ofoegbu et al. 2007). Considering the radial stress here is still very low and the rock is still under biaxial compression and it is ready to spall.

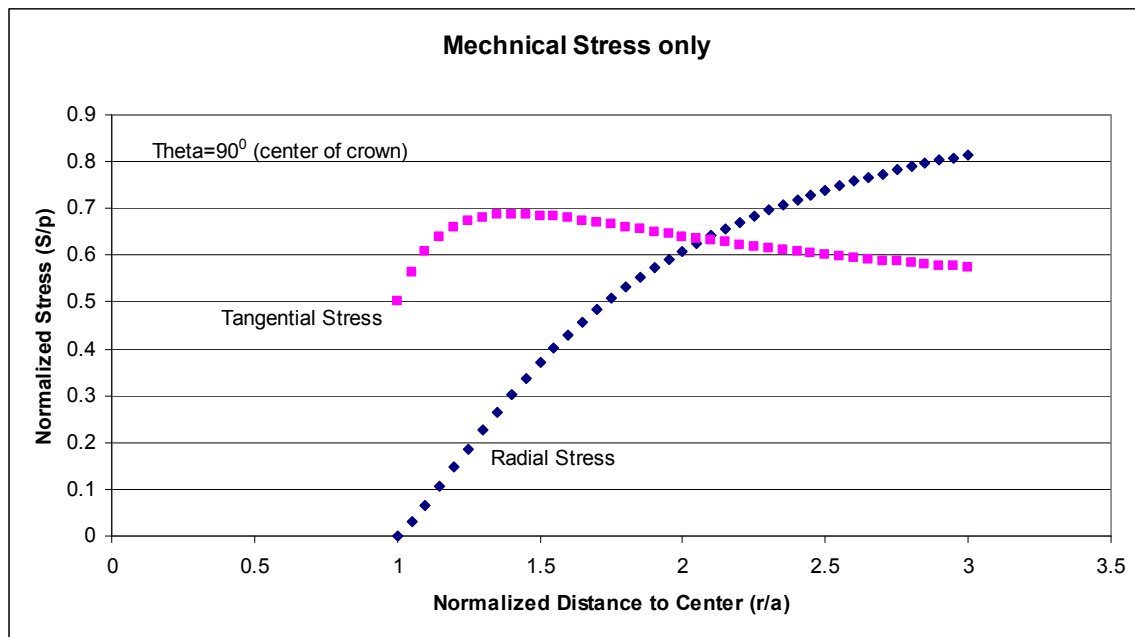


Figure 10. The tangential and radial mechanical stresses along the vertical line (Theta=90 degree, crown).

However, the tangential stress decreases quickly with increase distance. At r/a around 1.5 it is only about 1.7 time of the vertical stress, which is well below the uniaxial rock strength. The radial stress there is about the level of the vertical stress and the triaxial compressive rock strength here should be much higher than the tangential stress. At r/a near 2 the triaxial compressive rock strength is much higher than the tangential stress here for spalling to occur. Figure 12 shows the tangential thermoelastic stress near and around the drift opening, which is much higher than the uniaxial rock strength.

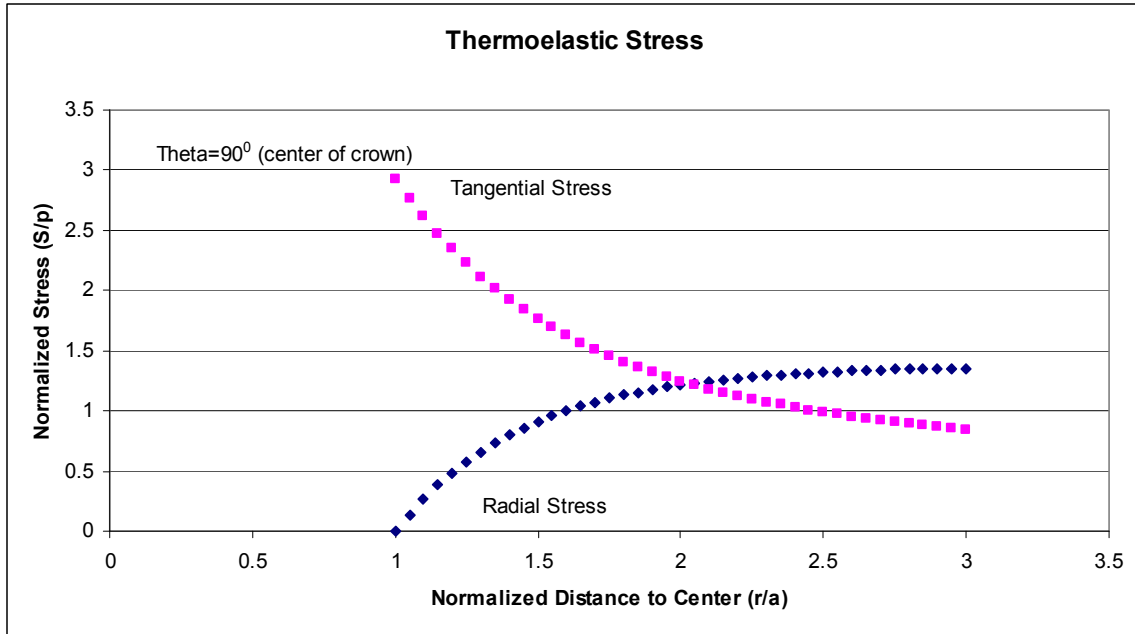


Figure 11. The tangential and radial thermoelastic stresses along the vertical line (Theta=90 degree, crown).

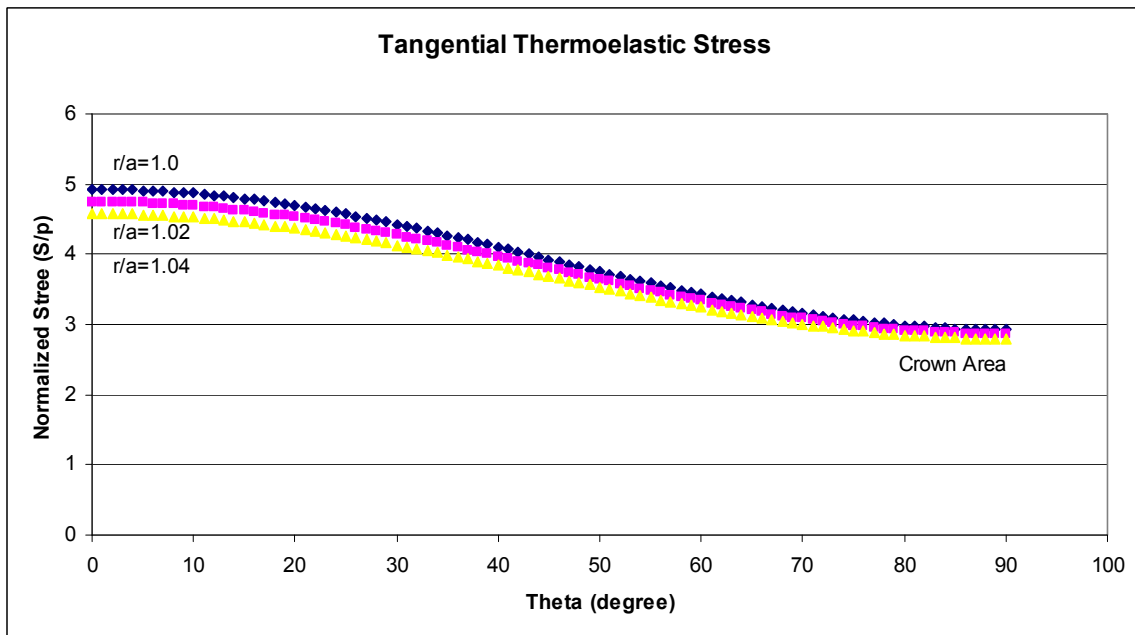


Figure 12. The tangential thermoelastic stress distribution near and around the drift opening.

Comparing Figs. 12 with 8, we see the stress difference between crown and sidewall areas is much smaller for the thermoelastic than for the pure mechanical. It is because the thermal stress is uniform and it also dominates.

If the crown area being heated more than other areas is considered, the curves in Fig. 12 should be even more flat. This means that in a modeling with homogeneous rock property a large area of the rock will spall at the same time. If a large time step Δt is used the small difference on stress will be smoothed out and make the area to spall at the same time even larger. This modeling process can completely eliminate the stress releasing process due to spalling itself in the lateral direction which plays an important role for spalling progressing deeper but not wider and stopping within two radiuses of the opening.

A simple analogy may help us to easily distinguish the differences between a homogeneous and a heterogeneous model here. If we assume a levee is homogeneous in strength, then the whole levee will break at the same time when a uniform load is exceeding the strength. But a heterogeneous levee will break at one or a few places first. The release of pressure due to the break at one or a few places will prevent more levee breaks. If multiple levees are lined up one after another, the homogeneous model will predict the whole levee breaks one after another; but the heterogeneous model will predict a few breaks on each levee. It is easy to see which model is physically reasonable.

(E) Abaqus Calculation of Post-Spalling Stress Distribution

In order to prove the lateral (tangential) stress release due to rock spalling we calculated the post-spalling stress distribution using the finite element software package Abaqus (V 6.9). The calculation is for the same tunnel configuration discussed in the previous sections.

The thermal loading is applied as a boundary condition to the tunnel opening, which follows the temperature history of Figure 6-30 (BSC, 2004). The temperature increases from about 30° C to about 40° C in 50 years and then increases to 150° C or 160° C in 10 years after repository closure. We let the high temperature continue for another 40 years in the modeling. Same temperature is assumed around the opening, which is similar to the temperature distribution shown in Figure 6-140 of BSC (2004). Manepally et al.'s (CNWRA, 2004) thermohydrological modeling showed that the temperature near crown area is about 20° C lower than the sidewall area at the highest temperature of postclosure and the difference decreases to almost zero at 10000 years of postclosure (Figure 2-2). Our choice of uniform thermal loading around the tunnel opening provides higher thermal stress at crown area than Manepally et al.'s model.

The theoretical calculation of the thermoelastic stress can be performed up to the point when there is a place meeting the rock failure criterion and spalling will occur. The following formula (Eq. E-4 in BSC, 2004) is adopted because it considers the strength change due to confine stress change or a triaxial stress-strength criterion:

$$\sigma_s = N\sigma_3 + \sigma_c$$

Where σ_s is the strength of the rock at failure, σ_3 is the confine pressure, σ_c is the unconfined compressive strength, and N is the confinement factor which obtained from test data (see Fig. E-2, BSC, 2004). The details of applying the above criterion are described in Appendix B. Using this criterion we find that an area spanning about 8° ($\theta = 90^\circ \pm 4^\circ$) near the opening at the crown area is first ready to spall.

So in the following we compare the post-spalling stress distribution for the configuration, in which two rows (about 10 cm thick) and four elements per row on each side of the vertical line at the crown area are removed (creating a notch), with the stress distribution for the configuration of nothing removed. Figure 13 is for nothing removed and Figure 14 is for the configuration to include a notch which simulates the first time spalling. In these two figures we plotted the Von Mises stress because it is a good measure for the stress condition using only one number.

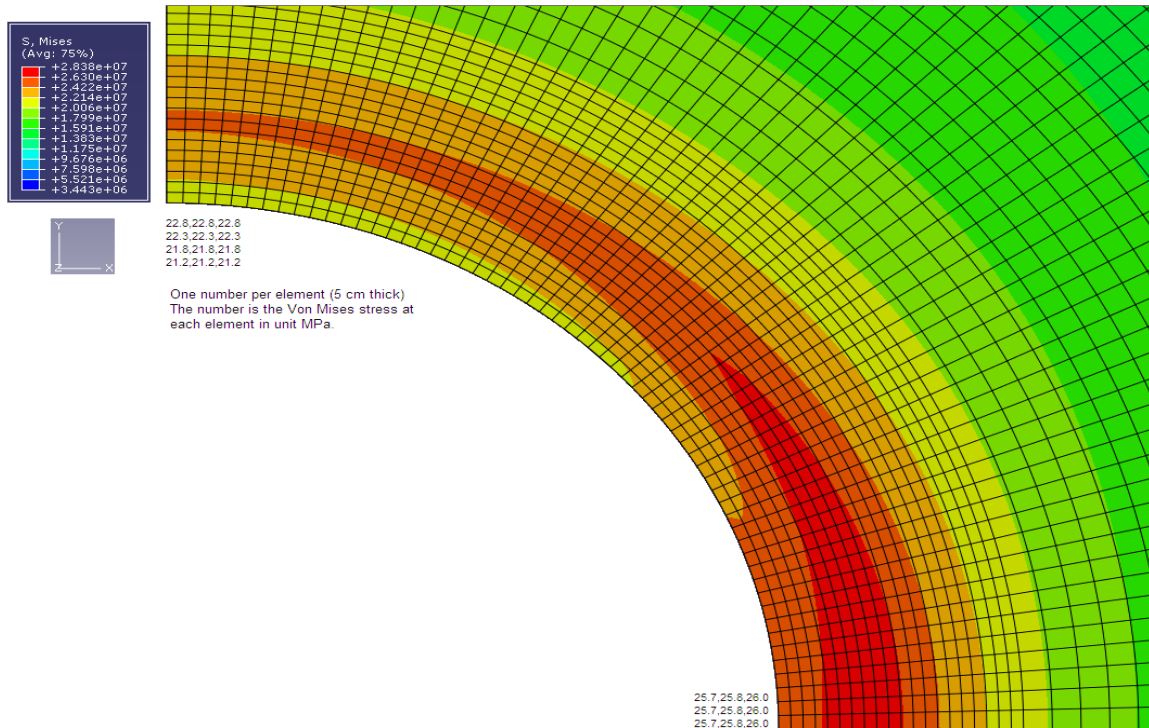


Figure 13. Stress distribution of the tunnel without spalling (no failure criterion is applied) after 100 years of thermal loading which reaches 160^o C and is kept for 40 years. The numbers near the crown and sidewall are Von Mises stress for those near by elements in unit of MPa.

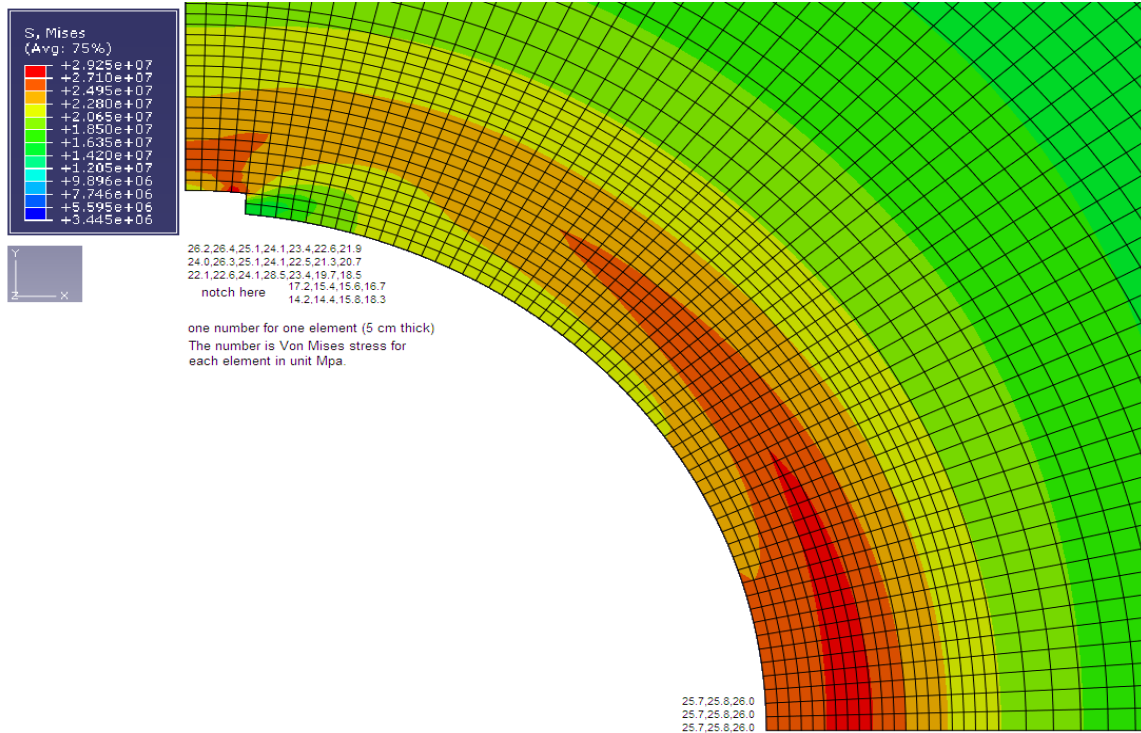


Figure 14. Stress distribution of the tunnel after the first time of spalling. The numbers near the notch and sidewall are Von Mises stress in unit of MPa for those near by elements.

The most interesting observation of the post spalling stress distribution (Fig. 14) is that the stress in the two rows near the opening starting from the notch is greatly released because of the spalling. The lowest stress is observed in the elements next to the notch which is about 14 to 17 MPa. It increases gradually toward the sidewall and reaches the same value around $\theta = 0^\circ$ as shown in Fig. 13. This stress release in lateral (tangential) directions due to spalling will stop the further spalling in the lateral directions even with further heating and only allows spalling going deeper.

The second observation is that the stress level above and near the notch is at the similar level of the crown area in Fig. 13. This is the area for the next spalling when the thermal stress increases.

(F) Discussion

When we compare the observational and modeling results described in the previous sections, we have the following tentative conclusions:

- 1) **Rock strength increases away from the opening.** Fig. 4 shows that the radial stress increases with increasing distance from the center or increases with the depth into the crown and sidewall. The immediate conclusion from this increase is that the rock strength should increase too.

This strength increase has recently being used by DOE in its RAI response (RAI: 3.2.2.1.2.1-003, page 1 of 9) to indicate that “the stresses greater than the unconfined compressive strength are not exactly at the boundary of the excavation, but at some distance from the boundary where the rock is stronger due to confinement.”

- 2) **Rock strength increase faster into the sidewall than into the crown.** It is very clear in Fig. 4 that the strength increase due to the confinement is much faster into the sidewall than into the crown. This may explain the observation (1) in section (A) and answer question (1) in section (A) why spalling occurs at the crown area instead of the sidewall area even the surface tangential stress at the former is lower than the latter.
- 3) **Confined rock strength a better measure for rock failure.** Combing the above analyses (1) and (2) it is easy to see why confined rock strength is a better measure for us to study drift degradation. This answers question (2) in section (A). The biaxial compression is the stress condition on the surface of the tunnel opening which is important to explain the spalling process very near the opening surface.
- 4) **Depth for maximum rock strength.** From Fig. 4 we see that the radial stress increases with the distance from the center of the tunnel and the two curves cross each other at about 1.7 radius and $0.5p$ for mechanical stress only. When the thermal stress is added it is at about two radiuses. Beyond this distance the rock strength returns to the level without excavation. This distance matches the observed worldwide spalling data on maximum spalling depth of one tunnel radius very well (question (3) in section (A)).
- 5) **Spalling process.** The conclusions we have reached on spalling are that (a) it shall start from two regions near crown and floor areas because the radial stress conditions in those two areas are most susceptible to spalling, (b) its extent should be smaller in dimension than the tunnel radius with a thickness of a few to ten percent of the radius, (c) spalling will start from a small area most susceptible to spalling and create a new area deeper into the rock for new spalling but releases tangential stress in the lateral (tangential) directions and prevents spalling extending in the lateral directions (not radial or deepening direction), (d) after multiple times of spalling and narrowing the spalling front becomes so small and deep into the well confined region with triaxial compressive strength a few time higher than the uniaxial unconfined strength the spalling stops and a cone shaped spalling region is created (Fig. 1).

The tangential stress in a ring about the thickness of the spalling depth should decrease to below the level that caused spalling to start. This ring is still going to provide some support and act as a heat barrier and prevent other part of the tunnel opening, which has not spalled, to spall. The crown part of the newly exposed rock is now under the similar mechanical and thermal stress loading like the part just spalled. It will spall again after enough time of thermal stress loading. This process will continue until stops within two radiuses from the center of opening (question (4) in section (A)).

- 6) **Thermal stress.** According DOE (BSC, 2004) and Ofoegbu et al. (2007) the thermal stress due to the tunnel heating will be the same level or higher than the mechanical stress. Our calculation confirms these results. So if the mechanical stress alone is not enough to start spalling the added thermal stress will start spalling. We have shown that heating mostly increases the tangential stress and slightly the radial stress. Because of the heterogeneity of rock strength spalling will occur at small area first and release the tangential stress preventing the extension of spalling laterally. Heating will speed up the spalling process but not enlarge the extent. The increased tangential stress is being released by spalling itself.

It will not cause significant increase in the total amount of rock spalling because this is controlled by how deep the spalling can go (about one radius from the opening). That thermal heating will speed up the spalling process but not increase the amount of spalling may have been observed in DOE's heating experiment. DOE's observation on the amount of rock spalled with heating matches the empirical formula (see RAI: 3.2.2.1.2.1-006, page 3 of 7) which was not from the data of spalling with heating.

According to a rough estimate of strength increase due to confining stress in 4) above and Fig. 2, the strength should increase to about three times of the unconfined uniaxial compressive strength within less than one radius from the crown. The total stress with thermal stress considered could reach about two to three times of the unconfined uniaxial compressive strength. So spalling should be stopped well within the distance of one radius from the free surface of the crown area under the predicted highest tunnel heating condition..

The major argument in this study is that spalling has to start from a small area due to heterogeneity or uneven loading. This means that the case of a large area being heated and loaded to reach the failure state at the same time and spall is impossible. Once spalling starts it releases the tangential stress in the inside ring and this ring will prevent spalling in the areas other than the area which has spalled. Continuing spalling is mostly going deeper from the previously spalled area not extending laterally because spalling creates similar stress conditions only in the deepening direction.

References

- Brady, B.H.G. and Brown, E.T. 1985, Rock mechanics for underground mining.
- BSC (Bechtel SAIC Company) 2004, Drift degradation analysis. ANL-EBS-MD-00027 REV 03 CAN 03 ERD 1. Las Vegas, Nevada: Bechtel SAIC Company.
- Kaiser, P.K., Diederichs, M.S., Martin, D., Sharpe, J. and Steiner, W. 2000, Invited keynote: Underground works in Hard rock tunneling and mining. GeoEng2000, Melbourne.
- Manepally, C., A. Sun, R. Fedors, and D. Farrell. Drift-Scale Thermohydrological Process Modeling-In Drift Heat Transfer and Drift Degradation, CNWRA 2004-5. San Antonio, Texas: CNWRA, 2004.
- Martin, R.J., Noel, J.S., Boyd, P.J., and Price, R.H. 1999, Creep and static fatigue of welded tuff from Yucca Mountain, Nevada, International Journal of rock mechanics and mining sciences, 34(3/4), 382. New York, New York: Elsevier.
- Ofoegbu, G.I., Smart, K.J., and Dasgupta, B. 2006, Assessing effects of thermal loading on the stability of emplacement drifts, Nuclear technology, Vol. 163.

Appendix A: Thermal Stress Formulation

The derivation of thermoelastic stress distribution around a circular tunnel with assumed temperature distribution

The general equation to be solved for distribution of thermoelastic stress for a two-dimensional problem (compatibility equation) is:

$$\nabla^4 \phi + E\alpha \nabla^2 T = 0 \quad (1)$$

Where ∇^2 denotes the two-dimensional Laplacian operator, ϕ is the stress potential that stress $\sigma_{ij} = \delta_{ij} \phi_{,kk} - \phi_{,ij}$, E , α , and T are Young's modulus, the coefficient of linear thermal expansion, and temperature respectively. Without the second term equation (1) is for the mechanical stress distribution only (no thermal) and its solution for a circular tunnel is the Kirsch solution. Now we want to solve equation (1) with assumed distribution of temperature. Because the opening is a circle we assume the temperature is only dependent on the distance (r) to the center of the opening. The opening radius is a .

Let

$$\phi = \phi^p + \phi^c \quad (2)$$

Where ϕ^p is any solution of (1) and then it is clear that it is also the solution of the following:

$$\nabla^2 \phi^p = -E\alpha T \quad (3)$$

With ϕ^p determined, ϕ^c is then the solution of the following constant-temperature problem (the Kirsch solution):

$$\nabla^4 \phi^c = 0 \quad (4)$$

We assume $T = T_0 a / r$ so at the opening surface ($r = a$) the temperature is at constant T_0 . This assumption of temperature only dependent on the distance to the center not on azimuth is an approximation because we know that the crown area is heated more than other areas. But we can choose a temperature for the crown area, which is higher than other areas, to be conservative. We have (3) in a cylindrical coordinate as:

$$\frac{d^2 \phi^p}{dr^2} + \frac{1}{r} \frac{d\phi^p}{dr} = -E\alpha T_0 a / r \quad (5)$$

This is a second order ordinary differential equation and can be easily solved. The solution is $\phi^p = D \ln(r) - Cr + F$, where D and F are arbitrary constants and $C = E\alpha T_0 a$. After solving for ϕ^p we can use the following equations to calculate the radial and tangential stresses of the thermal part:

$$\sigma_r^p = \frac{1}{r} \frac{d\phi^p}{dr} = D/r^2 - C/r \quad (6)$$

$$\sigma_\theta^p = \frac{d^2\phi^p}{dr^2} = -D/r^2 \quad (7)$$

But at $r = a$ the radial stress has to be zero so the constant D can be determined and we have:

$$\sigma_r^p = E\alpha T_0(a^2/r^2 - a/r) \quad (8)$$

$$\sigma_\theta^p = -E\alpha T_0 a^2/r^2 \quad (9)$$

These terms added to the Kirsch solution become the thermoelastic solution.

Appendix B: Criterion for Rock Failure

(1) The Kirsch formula will produce three 2D stresses (mechanical stresses)

$$\sigma_{rr}, \sigma_{\theta\theta}, \text{ and } \sigma_{r\theta}$$

For $\nu > 1/3$, they are all >0 at any place around the tunnel. The axial stress is σ_a ($= \nu(\sigma_{rr} + \sigma_{\theta\theta})$), where ν is the Poisson ratio, 0.2, see Geodynamics (Turcotte and Schubert, 1982) on page 110.

(2) The thermal and thermoelastic stresses are:

The thermal stresses are σ_r, σ_θ , and there is no thermal shear stress,

The thermoelastic stresses are

$$\sigma_{Tr} = \sigma_{rr} + \sigma_r$$

$$\sigma_{T\theta} = \sigma_{\theta\theta} + \sigma_\theta$$

$$\sigma_{Ts} = \sigma_{r\theta}$$

(3) To calculate the principal stresses in 2D (see eq. 2-43, page 83 of Turcotte and Schubert (1982)):

$$\sigma_{b,c} = \frac{\sigma_{Tr} + \sigma_{T\theta}}{2} \pm \left(\frac{(\sigma_{Tr} - \sigma_{T\theta})^2}{4} + \sigma_{Ts}^2 \right)^{1/2}$$

The axial stress is now $\sigma_a = \nu(\sigma_{Tr} + \sigma_{T\theta}) = \nu(\sigma_b + \sigma_c)$ if rigidly clamped.

(4) Order the three stresses σ_a , σ_b , and σ_c (if 2-D, σ_a is not needed)

$$\sigma_1 = \max(\sigma_a, \sigma_b, \sigma_c)$$

$$\sigma_3 = \min(\sigma_a, \sigma_b, \sigma_c)$$

(5) Rock failure strength

Calculate the confined rock strength Eq. E-4 on page 13 of Drift Degradation Analysis (BSC, 2004), #11 of DOE Ref)

$$\sigma_s = N\sigma_3 + \sigma_U$$

Where σ_s is the rock strength at failure, N is the confinement factor, σ_U is the unconfined compressive strength. For category 3 lithophysal (see Figure E-8 on page E-27 of Drift Degradation) $\sigma_U = 20MPa$. Using Eq. in Fig. E-2 (page E-16) and assuming the same slope as nonlithophysal, we have the failure strength:

$$\sigma_s = 7.72\sigma_3 + 20$$

(6) Failure criteria

$$\sigma_1 \geq \sigma_s$$

(7) end

(4) Order the three stresses σ_a , σ_b , and σ_c (if 2-D, σ_a is not needed)

$$\sigma_1 = \max(\sigma_a, \sigma_b, \sigma_c)$$

$$\sigma_3 = \min(\sigma_a, \sigma_b, \sigma_c)$$

(5) Rock failure strength

Calculate the confined rock strength Eq. E-4 on page 13 of Drift Degradation Analysis (BSC, 2004), #11 of DOE Ref)

$$\sigma_s = N\sigma_3 + \sigma_U$$

Where σ_s is the rock strength at failure, N is the confinement factor, σ_U is the unconfined compressive strength. For category 3 lithophysal (see Figure E-8 on page E-27 of Drift Degradation) $\sigma_U = 20MPa$. Using Eq. in Fig. E-2 (page E-16) and assuming the same slope as nonlithophysal, we have the failure strength:

$$\sigma_s = 7.72\sigma_3 + 20$$

(6) Failure criteria

$$\sigma_1 \geq \sigma_s$$

(7) end

ML102640197

| | | |
|---------------|----------|------------|
| OFFICE | HLWRS | HLWRS |
| NAME | T. Cao | J. Guttman |
| DATE | 09/21/10 | 09/22/10 |

OFFICIAL RECORD COPY